# Effect of (Cu-Ni) Concentrations Ratio on Recoverable Strain and the Shape Memory Effect of Ternary Smart (Cu-Al-Ni) Alloys

**MSc. Student Taher Mnajid Ammar**
**taher.mnajid69@gmail.com**
**Asst. prof. Dr. Ahmed Abdulrasool Alkhafaji**
**aa.alkhafaji@yahoo.com**
**University of Baghdad**
**Collage of engineering**
**Mechanical engineering department**

## Abstract: -

The achieved results by this research determined the best ratio of (Cu-Ni) in the smart (Cu-Al-Ni) alloys that it achieve the best values of maximum recoverable strain and shape memory effect. These mechanical properties possess great technological and commercial importance in many smart applications such as aerospace and industrial applications. Three samples have different weight percentage S1(82.8%Cu, 13.5%Al, 3.7%Ni), S2(81.8%Cu, 13.5%Al, 4.7%Ni) and S3(82.4%Cu, 13.5%Al, 4.1%Ni) were manufactured from smart (Cu-Al-Ni) alloy using powder metallurgy method with heat treatment. The physical tests were performed using optical microscope, scanning electron microscope (SEM) and X-ray diffraction (XRD) to make sure the presence of the austenite phase before heat treatment and the martensite after heat treatment. The results showed, the presence of these two phases in all samples under study. Mechanical tests were carried out which they included shape memory effect (SME) and maximum recoverable strain. The results showed that the S3 (82.4%Cu, 13.5%Al, 4.1%Ni) sample gave the best values of SME%, the maximum recoverable strain is 5% at full shape recovery (i.e. SME =100%), the maximum recoverable strain is 10% at partially shape recovery.

**Keywords: Powder metallurgy, recoverable strain (R.St.), shape memory effect (SME), smart (Cu-Al-Ni) alloys.**

## 1. Introduction

The smart alloys have the capability to recover their premier shape when they stimulated by an electrical current, thermo-mechanical, magnetic effects or any outer affect leads to raise their temperature above the transformation temperature, even if there are many plastic deformities **[5]**. These special characteristics of the smart alloys led to give them a great commercial and technological importance and use them in many diverse applications such as biomedical **[9]**, aerospace **[2]** &

industrial applications **[12]**. The smart alloys can be classified into many kinds, the NiTi alloy possesses the greatest number of applications, because of the limitations of this alloy such as the high expensive, it requires non-conventional machining and low transformation temperature (less than 100°C) therefore the best replacement particularly at the high transformation temperature is Cu-Al-Ni smart alloy since, it has lower cost, the easier manufacturing higher transformation temperature (-200°C to 200°C) and the maximum recoverable strain is 4% however it has some disadvantages such as the brittleness and the low corrosion resistance to treat them, they used powder metallurgy technique in which changing the percentage of the alloying elements or addition new elements or changing the conditions of heat treatment **[4 & 6]**. The phenomenon of thermoelastic martensitic transformation is the main responsible for the unique characteristics of smart alloys. Smart alloy possesses two major phases, low temperature phase and high temperature phase named as the martensite and the austenite. The start and finish temperatures of the martensite and austenite transformation are $M_s$, $M_f$, $A_s$, $A_f$. The shape memory effect is the attractive phenomenon in smart alloys in which the austenite phase cooled under $M_f$ temperature that lead to produce twinned martensite (zig zag form), its transform to detwinned martensite (orthorhombic) when the stress has been applied, but when the alloy is heated to a temperature upward $A_f$ after removing the stress, as a result that, the alloy returns to its original form as shown in **Fig.1**, **[8]**.

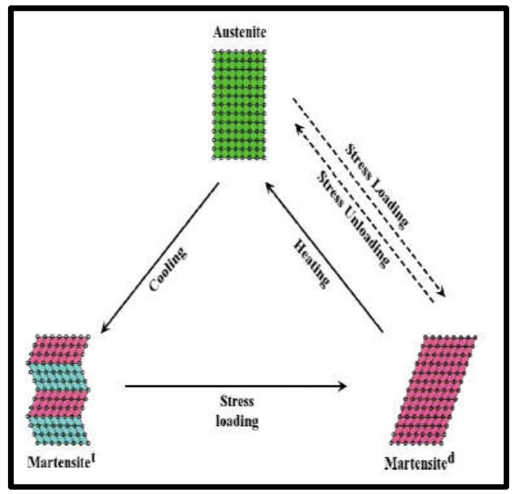


**Fig.1 The SME phenomenon in smart alloys [8]**

To study the Cu-Al-Ni smart alloys prefers selecting the ratios of Al between (13 to 14%) and Ni (1 to 6%) because they lead to obtain a single $\beta_3 \Longrightarrow \beta'_3$ martensite transformation, it causes particularly for high temperature applications, more thermoelastic & thermally more stable, but when the ratio of Al increases above (14%) lead to obtain single brittle phase $\gamma'_3$ it causes high brittleness of the smart alloy and its failure to restore its former shape as shown in **Fig. 2**, **[7]**. The purpose of this research was to study the effect of (Cu-Ni) ratio on the shape memory effect (strain recovery) and recoverable strain of ternary (Cu-Al-Ni) smart alloys, chosen ratios of the alloying elements depending on the comparison with the application of the new material CN-250X Nimesis alloy (single crystal wire) which it has (Cu 82.4wt%, Al 13.5wt%, Ni 4.1wt%) as shown in **Fig. 2**, recoverable strain (8 to 10%) for transformation temperature below 200°C was a better recoverable strain (6 to 7%) & transformation temperature (lower than 100°C) than NiTi **[3]**.

## 2. Experimental work

### 2.1. Pure powders

The used pure powders in this research were copper, aluminum and nickel possess the purity of 99.9 %, the mean particle sizes 45 micrometer (-325 mesh) and other specifications were shown in **Table.1 [10]**, they imported and was verified from the chemical composition by emission spectrometer device after compacting them by the uniaxial press machine with die and punches to manufacture sample was (14mm diameter & 5 mm thickness).

**Table.1 Specification of elements [10].**

| Specifications | Cu | Al | Ni |
|---|---|---|---|
| Density g/cm$^3$ | 8.94 | 2.685 | 8.902 |
| Melting temp. ºC | 1082 | 660 | 1455 |

### 2.2. Sample Preparation

Three different weight percentages S1(82.8%Cu, 13.5%Al, 3.7%Ni), S2(81.8%Cu, 13.5%Al, 4.7%Ni) and S3(82.4%Cu, 13.5%Al, 4.1%Ni) samples were manufactured with dimensions (16.5 mm length & 11mm diameter) from the smart (Cu-Al-Ni) alloy by using powder metallurgy technique. The manufacturing process was carried out according to the stages:

**2.2.1.** Mixing by 4-digits sensitive balance and rotating drum mixing device (shown in **Fig.3**) at speed 72 rpm for 6 hrs. The mixture is placed in the glass container at 40% of its volume to achieve the best mixing performance **[1]**, adding 1% acetone to prevent segregation between particles (because of the difference in the densities of the alloying elements) and for lubrication.

**2.2.2.** Compacting by a computerized uniaxial press machine (capacity of 100 KN) with floating die and punches (shown in **Fig.4**) at 650 Mpa, 4 minutes holding time (to prevent spring back) and 0.5 mm/min displacement rate to produce nine pieces of (16.5mm length * 11mm diameter) green compacts.

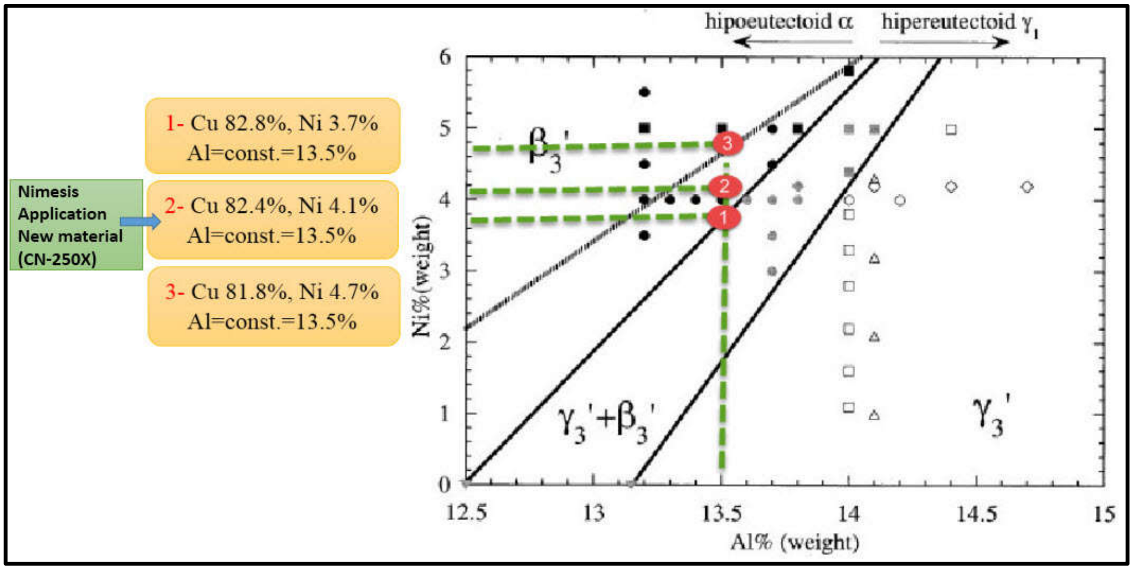


**Fig. 2 Three chosen Concentrations ratios of (Cu-Ni) for (Cu-Al-Ni) smart alloys were shown on diagram of the type of thermally induced martensite vs Al & Ni ratios [7]**

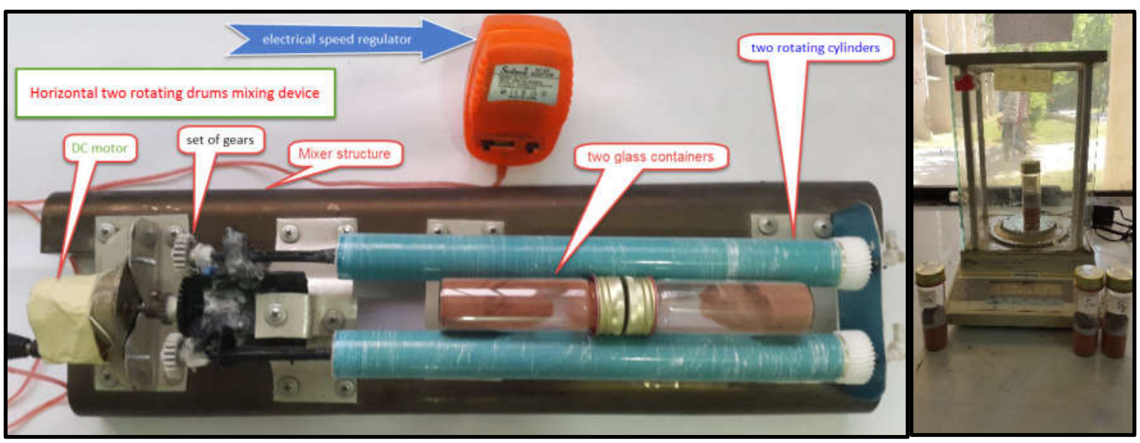


**Fig. 3 Rotating drum mixing device & 4-digits sensitive balance**


**Fig.4 Computerized uniaxial press machine, Dies & punches & green compacts**

**2.2.3.** Sintering by electrical furnace with a vacuum system to prevent the oxidation of the sample & disposal of harmful gases (shown in **Fig.5**). This process included two stages, it started at 500°C for one hour, then, it continued until 850°C for five hours, then let go it to cool in the furnace for the purpose of bonding particles of the sample in the solid state as shown in **Fig.6** [1]


**Fig.5 Electrical furnace with a vacuum system & sintered samples**

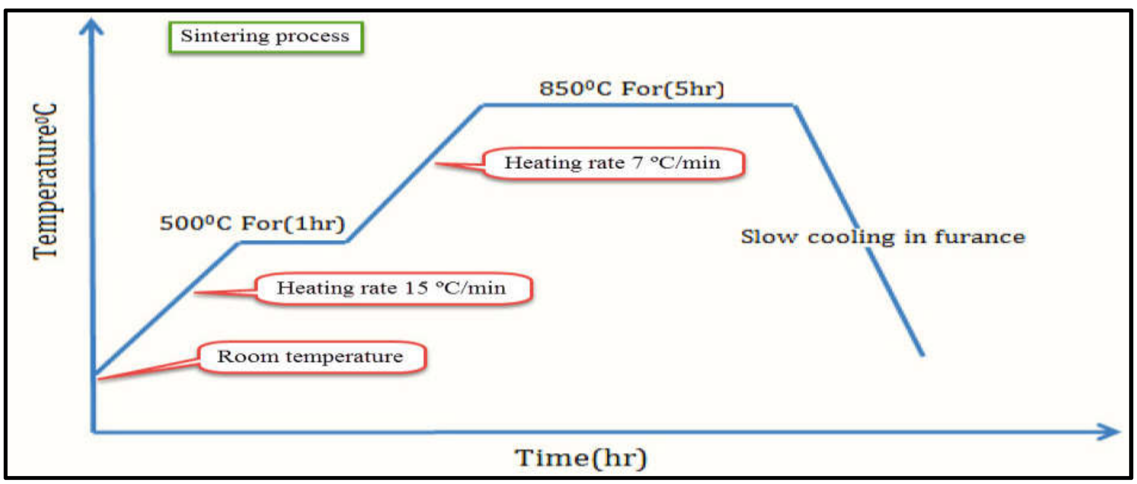


**Fig.6 Temperature- time diagram of sintering process steps**

**2.2.4.** Heat treatment using the same vacuum furnace system was used in sintering process. It included two stages: the first, quenching process in which the sample heated to 800°C, hold it for one hour, then cooled it speedily in ice water to obtain martensitic phase, the second, aging process in which the sample heated to 100°C, hold it for two hours, then cooled it in the air to guarantee the martensitic stabilization, as shown in **Fig.7.**

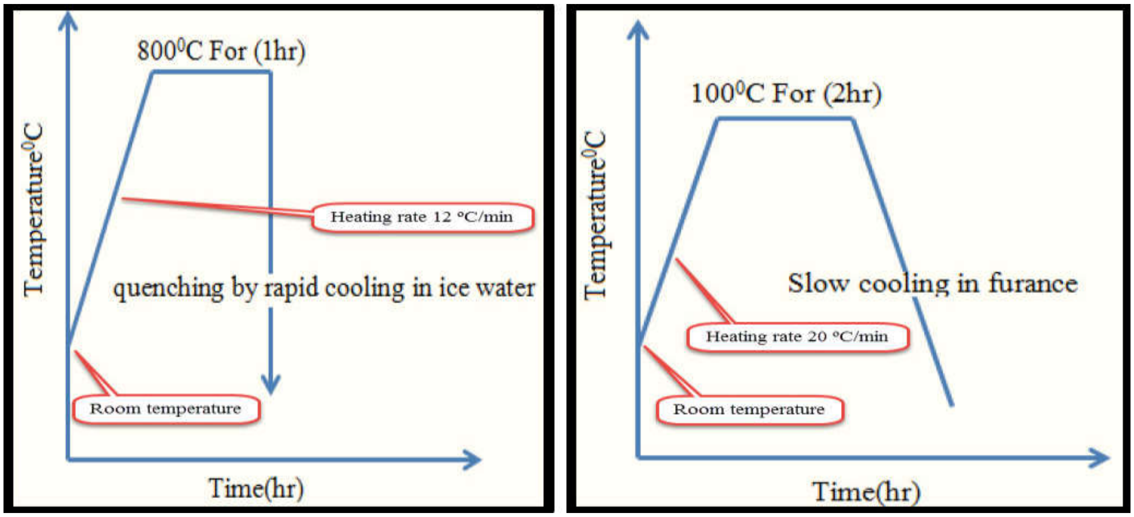


**Fig.7 Temperature- time diagram of (a) Quenching process & (b) Aging process**

**2.2.5.** Grinding, polishing and etching implemented on all samples to prepare them for physical and mechanical tests (shown in **Fig. 8**). The grinding was carried out by using a grinding device with two types of grinding paper and the water, the first, it was the waterproof aluminum oxide paper (400, 600, 800, 1200), the second, it was the waterproof silicon carbide paper (2000,3000) to remove the scratches and adjust straightness of the samples faces. The polishing was carried out by using polishing device with cloth paper and diamond paste to remove very fine surface scratches. The etching was carried out by using the chemical etching solution consist of the mixing (2 mg Fe3Cl, 5 ml HCl and 98 ml Ethanol).

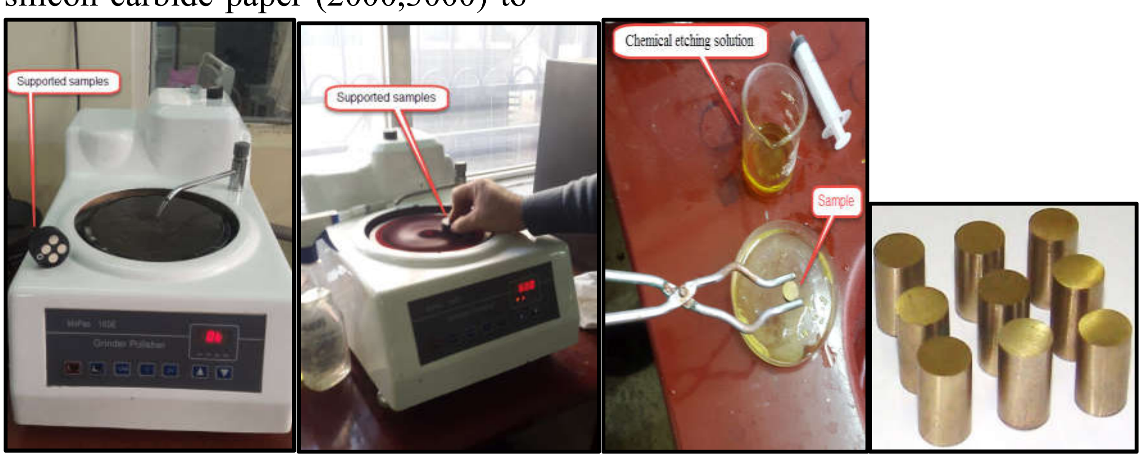


**Fig.8 Grinding, polishing, etching & finished samples.**

## 2.3. Testing

### 2.3.1 Physical Testing

The optical microscopic, X-ray Diffraction (XRD) & Scanning Electron Microscope (SEM) devices were used to determine the generated phases for each weight percentage of samples in order to make sure the austenite phase (Al4Cu9) present in the sintered samples, and the martensite phase (AlCu3) present in the quenched samples, because the main responsible of the SME phenomenon is the martensite phase.

### 2.3.2. Mechanical Testing

Recoverable strain (R.St.) and shape memory effect (SME) tests using the same vacuum furnace system previously used in the sintering process and press machine previously used in the compacting process. Initially, the sample was compacted by 1% from the original length, raised the temperature of it to 250 ° C, held it for a five minutes and left to cool in the air, then this procedure repeated several times by increasing recoverable strain at 1% for each step until the sample failed in restore the former shape or cracking it. The strain recovery ratio (SME%) was calculated by the equation **(1)**, **[11]**.

$$(\text{SME}\%) = \frac{L_2 - L_1}{L_0 - L_1} * 100\% \text{ --- } (1)$$

Where: $L_0$ *and* $L_1$ were the lengths before and after compacting, $L_2$ was the length after strain recovery (as a result of heating the compacted sample).

## 3. Results and Discussion

### 3.1. Optical Microscopic and (SEM) Tests Results

The testing results of optical microscopic and (SEM) devices for three samples of smart (Cu-Al-Ni) alloys that have different (copper-nickel) ratios are shown in two sets of images, the first set displayed austenite layers before heat treatment, and the second set displayed martensite layers (zig-zag or V-shape) after heat treatment as shown in **Fig. 9** and **Fig. 10**.

### 3.2. XRD Test Results

**Fig. 11** shows the XRD test results of (S1, S2 & S3) samples, this results were demonstrated the presence of the austenite phase (Al4Cu9) in the sintered samples and the martensite phase (AlCu3) in the quenched samples.

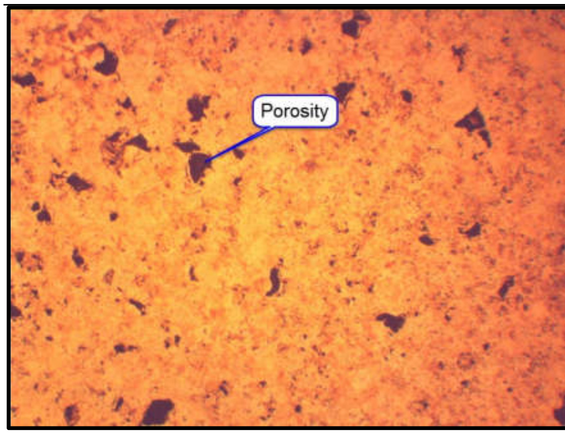


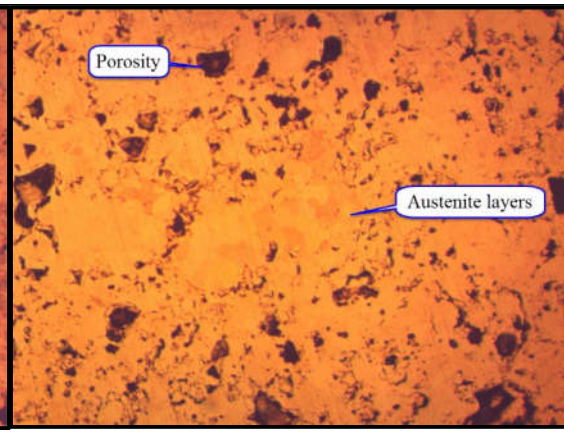


**S1 sample - before heat treatment** **S2 sample - before heat treatment**

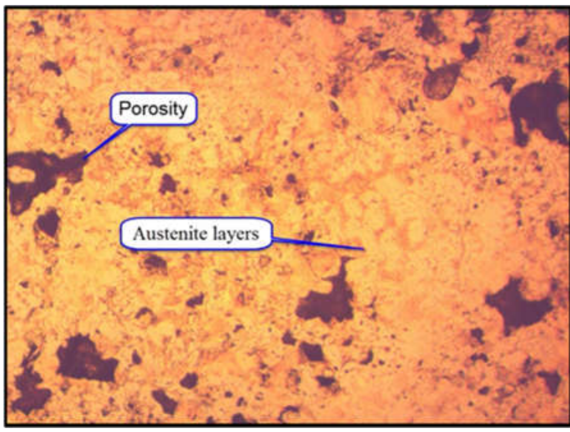


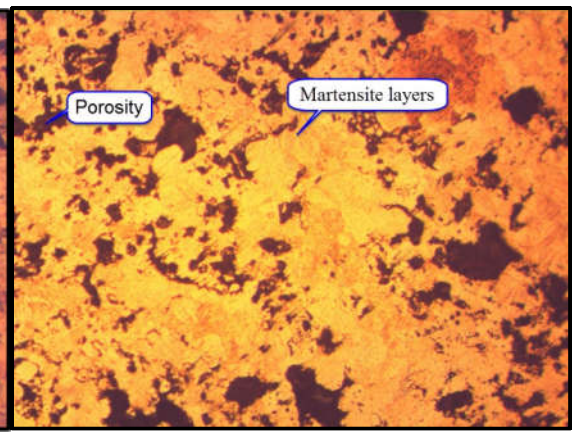


**S3 sample - before heat treatment** **S1 sample - after heat treatment**

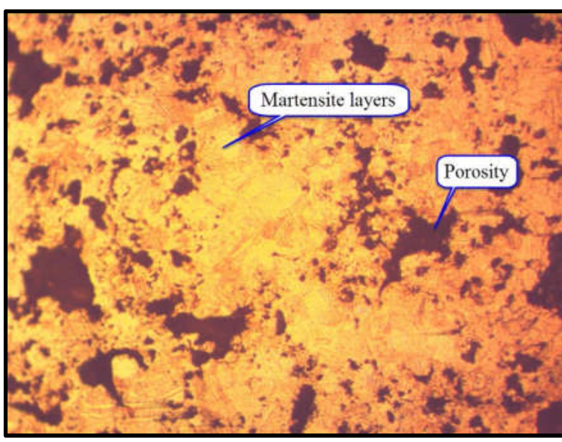


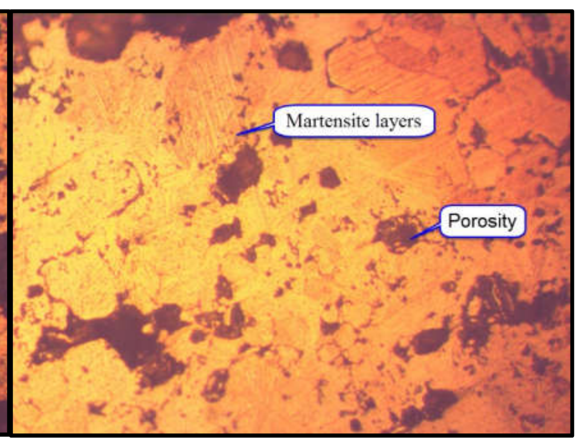


**S2 sample - after heat treatment** **S3 sample - after heat treatment**

**Fig. 9 Optical microscopic test images (magnification power 40X)**

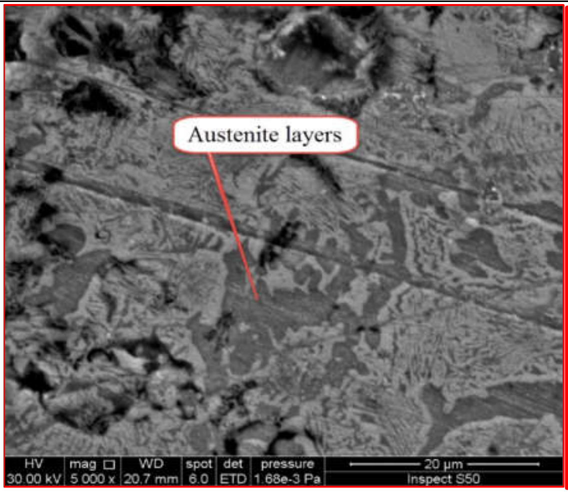


S1 sample - before heat treatment

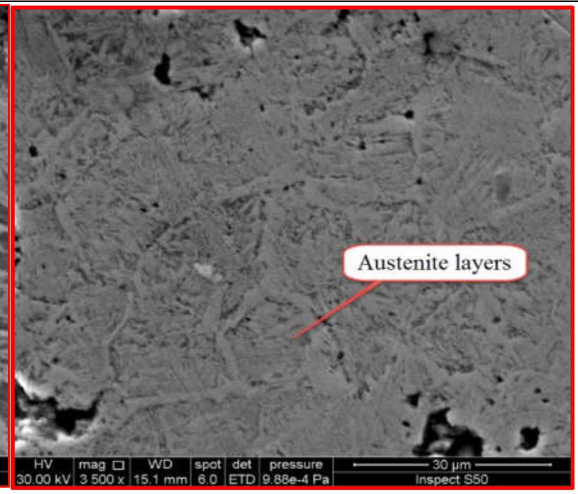


S2 sample - before heat treatment

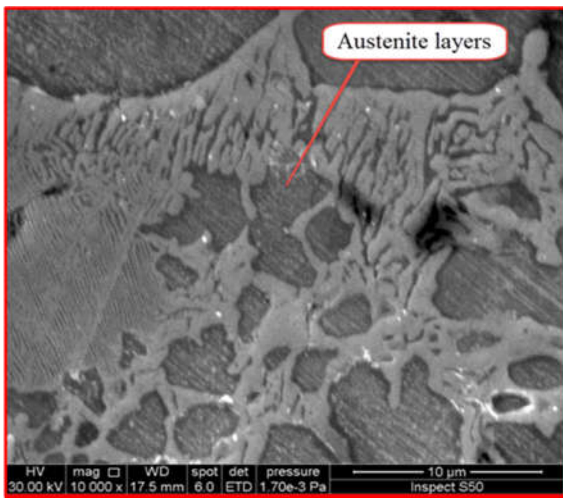


S3 sample - before heat treatment

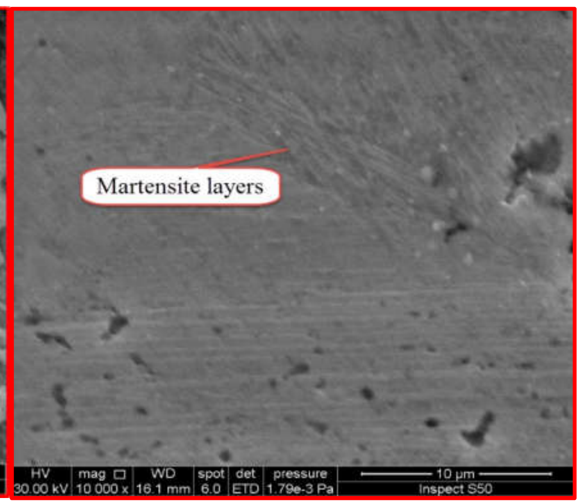


S1 sample - after heat treatment

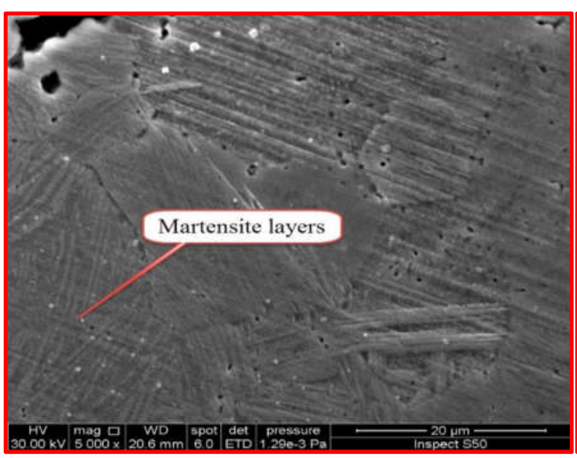


S2 sample - after heat treatment

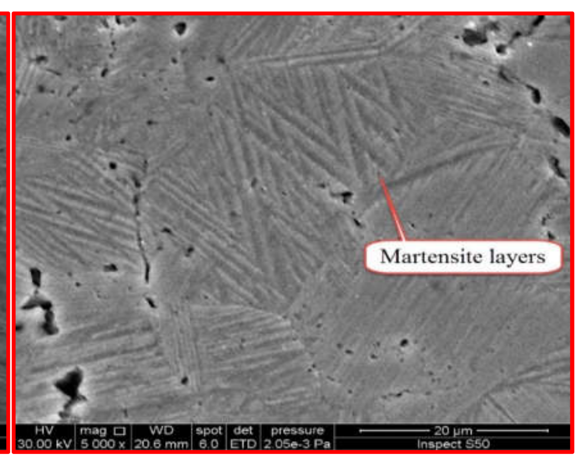


S3 sample - after heat treatment

**Fig. 10 Scanning Electron Microscope (SEM) test images (magnification 3500X-10000X)**

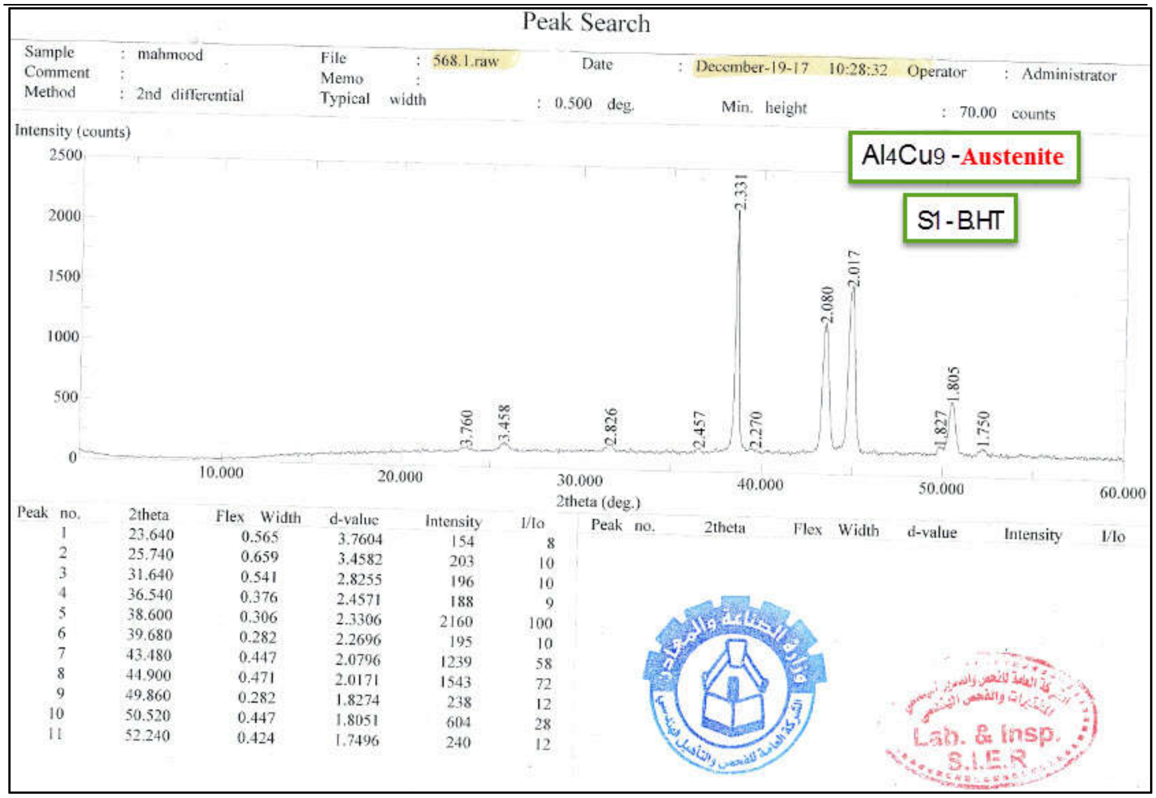


| Peak no. | 2theta | Flex Width | d-value | Intensity | I/Io |
|---|---|---|---|---|---|
| 1 | 23.640 | 0.565 | 3.7604 | 154 | 8 |
| 2 | 25.740 | 0.659 | 3.4582 | 203 | 10 |
| 3 | 31.640 | 0.541 | 2.8255 | 196 | 10 |
| 4 | 36.540 | 0.376 | 2.4571 | 188 | 9 |
| 5 | 38.600 | 0.306 | 2.3306 | 2160 | 100 |
| 6 | 39.680 | 0.282 | 2.2696 | 195 | 10 |
| 7 | 43.480 | 0.447 | 2.0796 | 1239 | 58 |
| 8 | 44.900 | 0.471 | 2.0171 | 1543 | 72 |
| 9 | 49.860 | 0.282 | 1.8274 | 238 | 12 |
| 10 | 50.520 | 0.447 | 1.8051 | 604 | 28 |
| 11 | 52.240 | 0.424 | 1.7496 | 240 | 12 |

**S1 sample – XRD test, Austenite phase (Al4Cu9) before heat treatment**

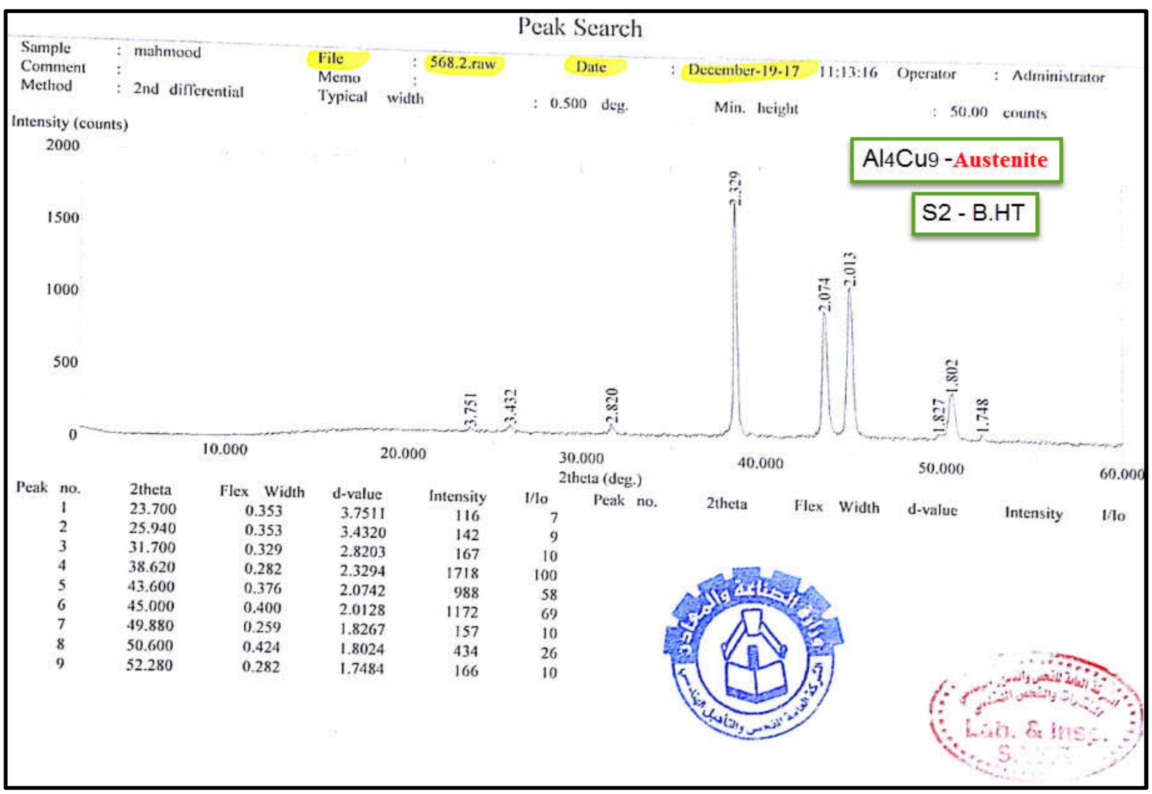


| Peak no. | 2theta | Flex Width | d-value | Intensity | I/Io |
|---|---|---|---|---|---|
| 1 | 23.700 | 0.353 | 3.7511 | 116 | 7 |
| 2 | 25.940 | 0.353 | 3.4320 | 142 | 9 |
| 3 | 31.700 | 0.329 | 2.8203 | 167 | 10 |
| 4 | 38.620 | 0.282 | 2.3294 | 1718 | 100 |
| 5 | 43.600 | 0.376 | 2.0742 | 988 | 58 |
| 6 | 45.000 | 0.400 | 2.0128 | 1172 | 69 |
| 7 | 49.880 | 0.259 | 1.8267 | 157 | 10 |
| 8 | 50.600 | 0.424 | 1.8024 | 434 | 26 |
| 9 | 52.280 | 0.282 | 1.7484 | 166 | 10 |

**S2 sample – XRD test, Austenite phase (Al4Cu9) before heat treatment**

Peak Search

Sample : mahmood File : 568.3.raw Date : December-19-17 11:57:56 Operator : Administrator
Comment : Memo :
Method : 2nd differential Typical width : 0.500 deg. Min. height : 60.00 counts

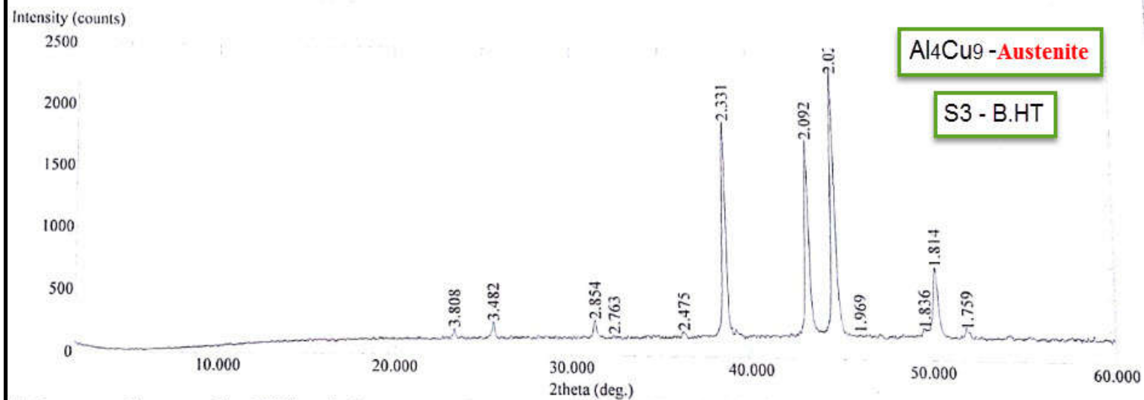


| Peak no. | 2theta | Flex Width | d-value | Intensity | I/Io |
|---|---|---|---|---|---|
| 1 | 23.340 | 0.282 | 3.8081 | 209 | 10 |
| 2 | 25.560 | 0.282 | 3.4822 | 262 | 12 |
| 3 | 31.320 | 0.282 | 2.8537 | 282 | 13 |
| 4 | 32.380 | 0.259 | 2.7626 | 167 | 8 |
| 5 | 36.260 | 0.282 | 2.4754 | 201 | 9 |
| 6 | 38.600 | 0.306 | 2.3306 | 1896 | 83 |
| 7 | 43.220 | 0.306 | 2.0915 | 1751 | 77 |
| 8 | 44.660 | 0.306 | 2.0274 | 2285 | 100 |
| 9 | 46.060 | 0.259 | 1.9690 | 203 | 9 |
| 10 | 49.620 | 0.259 | 1.8357 | 249 | 11 |
| 11 | 50.240 | 0.353 | 1.8145 | 736 | 33 |
| 12 | 51.940 | 0.306 | 1.7590 | 243 | 11 |

Peak no. 2theta Flex Width d-value Intensity I/Io

Lab. & Insp.

**S3 sample – XRD test, Austenite phase (Al4Cu9) before heat treatment**

**S1 sample – XRD test, Martensite phase (AlCu3) after heat treatment**

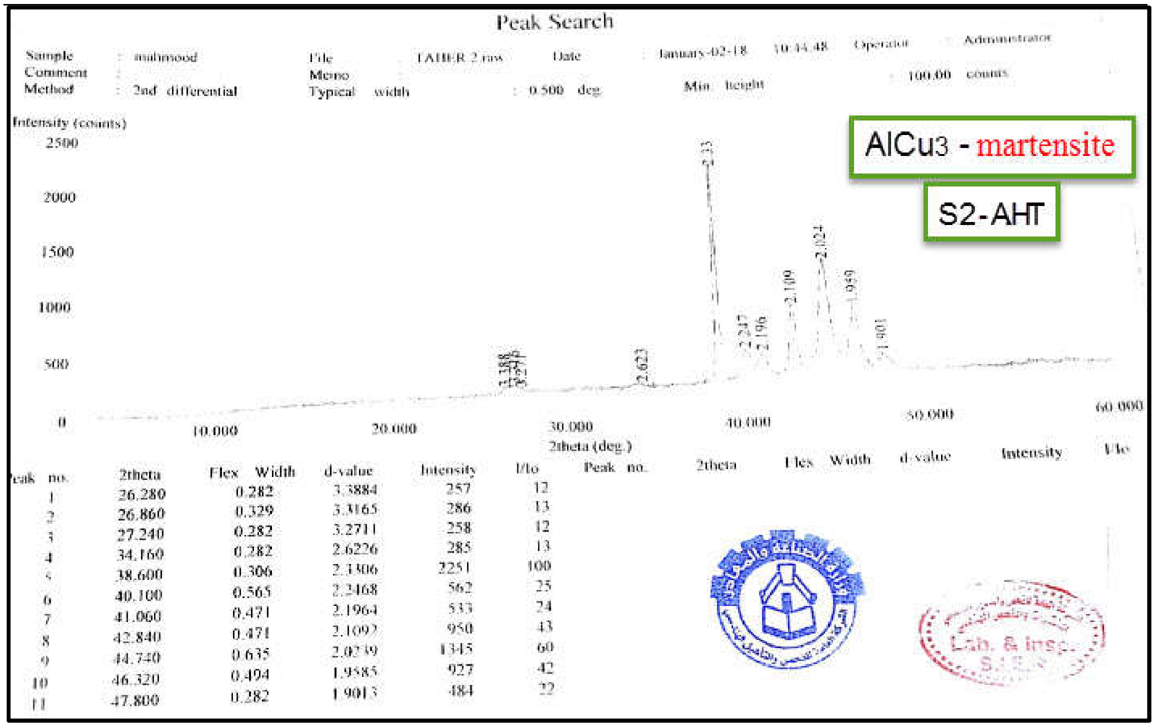


| Peak no. | 2theta | Flex Width | d-value | Intensity | I/Io |
|---|---|---|---|---|---|
| 1 | 26.280 | 0.282 | 3.3884 | 257 | 12 |
| 2 | 26.860 | 0.329 | 3.3165 | 286 | 13 |
| 3 | 27.240 | 0.282 | 3.2711 | 258 | 12 |
| 4 | 34.160 | 0.282 | 2.6226 | 285 | 13 |
| 5 | 38.600 | 0.306 | 2.3306 | 2251 | 100 |
| 6 | 40.100 | 0.565 | 2.2468 | 562 | 25 |
| 7 | 41.060 | 0.471 | 2.1964 | 533 | 24 |
| 8 | 42.840 | 0.471 | 2.1092 | 950 | 43 |
| 9 | 44.740 | 0.635 | 2.0239 | 1345 | 60 |
| 10 | 46.320 | 0.494 | 1.9585 | 927 | 42 |
| 11 | 47.800 | 0.282 | 1.9013 | 484 | 22 |

**S2 sample – XRD test, Martensite phase (AlCu3) after heat treatment**

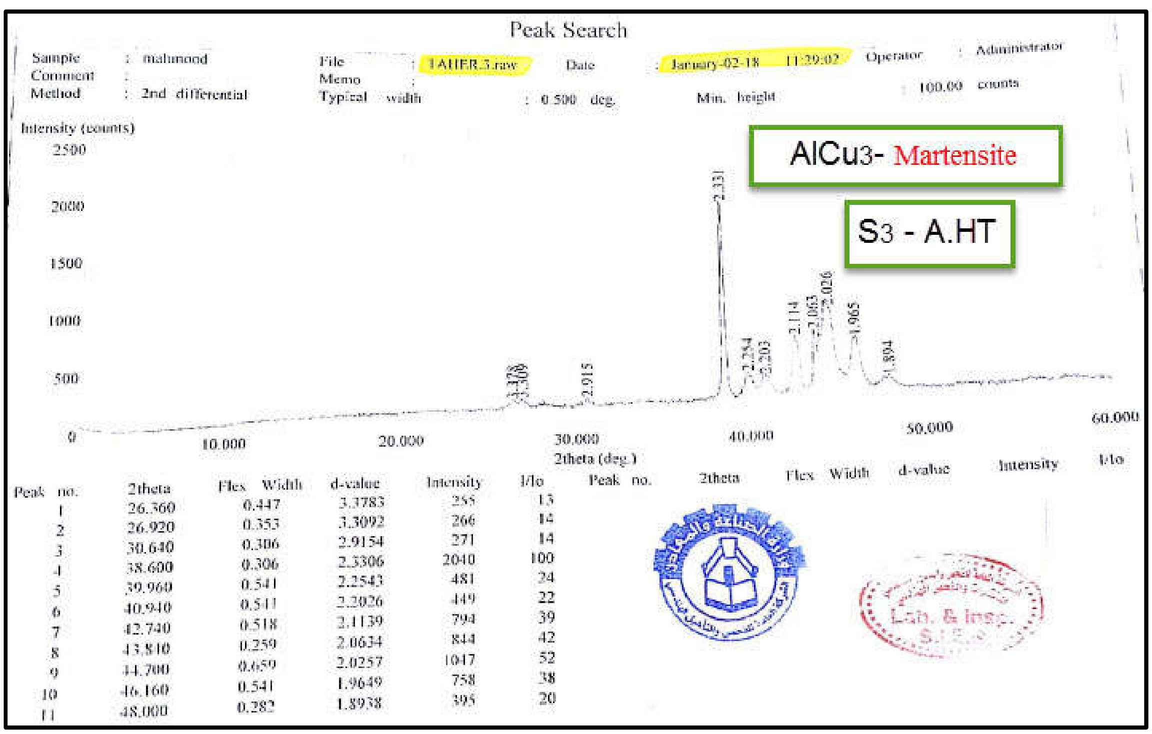


| Peak no. | 2theta | Flex Width | d-value | Intensity | I/Io |
|---|---|---|---|---|---|
| 1 | 26.360 | 0.447 | 3.3783 | 255 | 13 |
| 2 | 26.920 | 0.353 | 3.3092 | 266 | 14 |
| 3 | 30.640 | 0.306 | 2.9154 | 271 | 14 |
| 4 | 38.600 | 0.306 | 2.3306 | 2040 | 100 |
| 5 | 39.960 | 0.541 | 2.2543 | 481 | 24 |
| 6 | 40.940 | 0.541 | 2.2026 | 449 | 22 |
| 7 | 42.740 | 0.518 | 2.1139 | 794 | 39 |
| 8 | 43.810 | 0.259 | 2.0634 | 844 | 42 |
| 9 | 44.700 | 0.659 | 2.0257 | 1047 | 52 |
| 10 | 46.160 | 0.541 | 1.9649 | 758 | 38 |
| 11 | 48.000 | 0.282 | 1.8938 | 395 | 20 |

**S3 sample – XRD test, Martensite phase (AlCu3) after heat treatment**

**Fig. 11 X-ray Diffraction (XRD)test images**

### 3.3. Recoverable strain and Shape Memory Effect Testing Results

The results of this testing were shown in the **Table 2**.

**Table 2. Recoverable strain and shape Memory effect testing results**

| | | | | |
|---|---|---|---|---|
| ($S_1$) Sample – [82.8%Cu, 13.5%Al, 3.7%Ni] | | | | |
| R.St.% (mm) | $L_o$ (mm) | $L_1$ (mm) | $L_2$ (mm) | SME% (mm) |
| 1 % $L_o$ | 16.575 | 16.570 | 16.575 | 100 |
| 2 % $L_o$ | 16.575 | 16.540 | 16.575 | 100 |
| 3 % $L_o$ | 16.575 | 16.495 | 16.575 | 100 |
| 4 % $L_o$ | 16.575 | 16.440 | 16.560 | 88.889 |
| 5 % $L_o$ | 16.560 | 16.355 | 16.490 | 65.854 |
| 6 % $L_o$ | 16.490 | 15.960 | 16.260 | 56.604 |
| 7 % $L_o$ | 16.260 | 15.840 | 16.050 | 50 |
| 8 % $L_o$ | 16.050 | 15.630 | 15.830 | 47.62 |
| 9 % $L_o$ | 15.830 | 15.230 | 15.480 | 41.667 |
| 10 % $L_o$ | 15.480 | 14.920 | 15.050 | 23.214 |
| 11 % $L_o$ | 15.050 | 14.430 | 14.510 | 12.903 |
| 12 % $L_o$ | 14.510 | Failure | Failure | Failure |
| ($S_2$) Sample – [81.8%Cu, 13.5%Al, 4.7%Ni] | | | | |
| R.St. % (mm) | $L_o$ (mm) | $L_1$ (mm) | $L_2$ (mm) | SME% (mm) |
| 1 % $L_o$ | 15.480 | 15.475 | 15.480 | 100 |
| 2 % $L_o$ | 15.480 | 15.463 | 15.480 | 100 |
| 3 % $L_o$ | 15.480 | 15.430 | 15.480 | 100 |
| 4 % $L_o$ | 15.480 | 15.400 | 15.480 | 100 |
| 5 % $L_o$ | 15.480 | 15.350 | 15.455 | 80.77 |
| 6 % $L_o$ | 15.455 | 15.180 | 15.380 | 72.727 |
| 7 % $L_o$ | 15.380 | 14.830 | 15.090 | 47.273 |
| 8 % $L_o$ | 15.090 | 14.730 | 14.890 | 44.444 |
| 9 % $L_o$ | 14.890 | 14.400 | 14.610 | 42.857 |
| 10% | 14.610 | 14.120 | 14.290 | 34.7 |
| 11% | 14.290 | Failure | Failure | Failure |
| ($S_3$) Sample – [82.4%Cu, 13.5%Al, 4.1%Ni] | | | | |
| R.St. % (mm) | $L_o$ (mm) | $L_1$ (mm) | $L_2$ (mm) | SME% (mm) |
| 1 % $L_o$ | 15.220 | 15.216 | 15.220 | 100 |
| 2 % $L_o$ | 15.220 | 15.200 | 15.220 | 100 |
| 3 % $L_o$ | 15.220 | 15.165 | 15.220 | 100 |
| 4 % $L_o$ | 15.220 | 15.140 | 15.220. | 100 |
| 5 % $L_o$ | 15.220 | 15.060 | 15.220 | 100 |
| 6 % $L_o$ | 15.220 | 14.800 | 15.180 | 90.476 |
| 7 % $L_o$ | 15.180 | 14.700 | 15.110 | 85.417 |
| 8 % $L_o$ | 15.110 | 14.660 | 15.010 | 77.777 |
| 9 % $L_o$ | 15.010 | 14.380 | 14.690 | 49.206 |
| 10 % $L_o$ | 14.690 | 14.150 | 14.390 | 44.444 |
| 11 % $L_o$ | 14.390 | Failure | Failure | Failure |

These results were represented in **Fig. 12**.

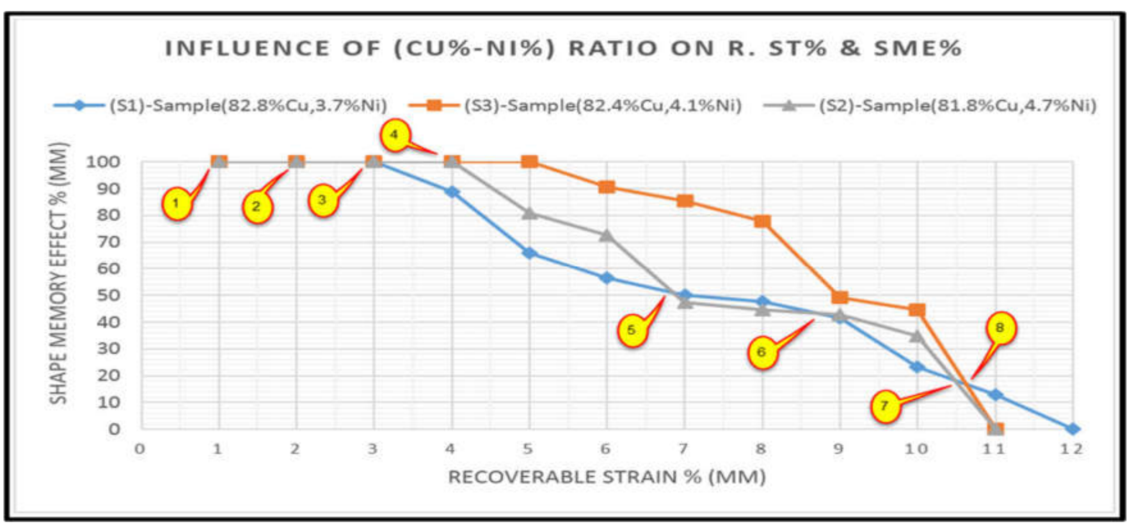


**Fig. 12 Graph shows the effect of changing in (Cu-Ni) ratio with constant Al% on recoverable strain and shape memory effect in smart (Cu-Al-Ni) alloys**

The (SME% – R.St.%) curves of the (S1, S2 & S3) samples in **Fig. 12** shows:

1- When increasing (R. St %) due to increasing the applied force, the (SME%) decreases for all samples.

2- The sample (S3) gave the (SME%) greater than the (SME%) of the samples ($S_1$ & $S_2$) when increasing the (R. St %).

3- The sample ($S_3$) gave the greatest (maximum recoverable strain = 5%) at full shape recovery, (maximum recoverable strain =10%) at partially shape recovery

4- The intersection points (1,2,3,5,6 &7) between the curves of S1 and S2 samples, the intersection points (1,2,3 & 4) between the S2 and S3 samples curves and the intersection points (1,2,3 & 8) between the S1 and S3 samples curves indicate that the samples behavior is similar at these intersection points.

In **Fig. 9** and **Fig. 10**, observed after heat treatment of S1, S2 and S3 samples appearance martensitic layers (V-shape) very weak in S1(82.8%Cu, 13.5%Al, 3.7%Ni) sample which it possesses least value of nickel concentration among three samples. In **Table 2** and **Fig. 12,** S1 sample gave the least value of (maximum recoverable strain = 3%) at full shape recovery and also gave the lowest values of (SME%) among the three samples. Because when decreasing nickel concentration at constant aluminum concentration that lead to instability of single martensitic phase β3 and decrease single martensitic layers β3 (where the martensitic transformation changes from single ($\beta_3 \Longrightarrow \beta'_3$) to mixed ($\beta_3 \Longrightarrow \beta'_3 + \gamma'_3$) as shown in **Fig. 2**. The appearance of the brittle phase $\gamma'_3$ cause increasing the brittleness of the (Cu-Al-Ni) alloy and lead to decrease shape recovery characteristics (recoverable strain and shape memory effect). The major cause of the SME and other shape recovery properties is the stability of the β phase with a cubic structure. Where, it is believed that addition of nickel slows the diffusion of copper and aluminum.

## 4. Conclusions

From the results analysis for the samples testing ($S_1$, $S_2$ & $S_3$) we conclude

1- The values of (R.St.% & SME%) increased with increasing Ni% (from 3.7 to 4.1) and decreasing (Cu%). The (R.St.% & SME%) began to decrease after the Ni% increased to above 4.1%.

2- The sample S3 which it possesses the chemical composition (82.4%Cu, 13.5%Al, 4.1%Ni) was the best among the three samples because it achieved the greatest recoverable strain ratio (5%) at full shape recovery (SME=100%).

3- The sample ($S_1$) gave the greatest (R.St.=11%) at partially shape recovery, but it not preferred because it gave the least value of (R. St.=3%) at full shape recovery and also gave the lowest values of (SME%) among the three samples when increasing the (R.St. %), because it has the least value of nickel concentration (3.7% Ni).

4- There is the greatest convergence of behavior between the S1 (82.8%Cu, 13.5%Al, 3.7%Ni) sample and S2 (81.8%Cu, 13.5%Al, 4.7%Ni) sample in the shape recovery property because the number of intersection points between their curves (6 points) are more than the intersection points (4 points) with other.

## 5. References

1. Groover, M. P.” Fundamentals of Modern Manufacturing Materials, Processes, and Systems” John Wiley & Sons, part IV, chapter 15, p 375-399, (2013) Fifth Edition.

2. Hartl D. J., & Lagoudas D. C., “Aerospace Applications of Shape Memory Alloys”, Part G: Journal of Aerospace Engineering, Vol. 221, Issue 4, pp. 535-552, (2007).

3. Hautcoeur A., Fouché, F. & Sicre, J., “Cu-Al-Ni Shape Memory Single Crystal Wires with High Transformation Temperature” 16th European Space Mechanisms and Tribology Symposium 2015, Bilbao, Spain, p. 23–25, (2016).

4. Hodgson D. E., Ming W. H., & Biermann R. J., “Shape Memory Alloys” ASM International, Metals Handbook, Tenth Edition, Vol. 2, pp. 897-902, (1990).

5. Kolekar A., Natak A., Navratne K. and Mali A., “Recent Advancement in Shape Memory Alloy”, International Research Journal of Engineering and Technology (IRJET), Vol. 4, Issue 4, pp. 2120-2125, (2017).

6. Rajeshkumar R., & ME T. Vigraman, “Formation of Cu-Al-Ni Shape Memory Alloy with the Addition of Alloying Elements Mn and Si”, International journal of scientific and engineering research, Vol. 5, Issue 5, pp.179-182, (2014).

7. Recarte V., Pérez-Sáez, R. B., San Juan, J., Bocanegra, E. H., & Nó, M. L., "Influence of Al and Ni Concentration on the Martensitic Transformation in Cu-Al-Ni Shape Memory Alloys." Metallurgical and Materials Transactions A, Vol. 33, No. 8, pp. 2581-2591, (2002).

8. Rigamonti D. & Zanetti F., “Design and Characterization of Shape Memory Alloys for Optomechanical Mounting”, Polytechnic of Milan, Faculty of

industrial engineering degree course in space engineering academic, (Dissertation) pp.6-9, (2012).

9. Petrini L., & Migliavacca F., "Biomedical Applications of Shape Memory Alloys", Hindawi Publishing Corporation, Journal of Metallurgy, Vol. 2011, Article ID 501483, pp. 1-15, (2011).

10. Schwartz M., "Smart Materials-Encyclopedia of Materials, Parts and Finishes", CRC Press, Library of Congress, Second Edition, (2002).

11. Wan J., Huang X., Chen S., & TY H. X. Z. "Effect of Nitrogen Addition on Shape Memory Characteristics of Fe-Mn-Si-Cr Alloy", Materials transactions, Vol. 43, No. 5, pp. 920-925, 2002.

12. Wu M. H., & Schetky L. M., "Industrial Applications for Shape Memory Alloys" Proceedings of the International Conference on Shape Memory and Super-elastic Technologies, Pacific Grove, California, Vol. 44, No. 1, pp.171-182 (2000).

# تأثير نسبة تراكيز (نحاس-نيكل) على الانفعال القابل للاستعادة وتأثير ذاكرة الشكل لسبيكة (نحاس-المنيوم-نيكل) الثلاثية الذكية

**طالب الماجستير: طاهر مناجد عمار**
**taher.mnajid69@gmail.com**
**الأستاذ المساعد الدكتور: أحمد عبد الرسول الخفاجي**
**aa.alkhafaji@yahoo.com**
**جامعة بغداد**
**كلية الهندسة**
**قسم الهندسة الميكانيكية**

## الخلاصة:-

حددت النتائج المتحققة بواسطة هذا البحث أفضل نسبة (نحاس-نيكل) في سبائك (نحاس - المنيوم - نيكل) الذكية التي تحقق أفضل القيم لاعظم انفعال قابل للاستعادة وتأثير ذاكرة الشكل. هذه الخواص الميكانيكية تملك اهمية تجارية وتكنولوجية كبيرة في الكثير من التطبيقات الذكية مثل تطبيقات الفضاء والتطبيقات الصناعية. ثلاثة عينات لها نسب وزنية مختلفة S1 ( 82,8% نحاس, 13,5% المنيوم, 3,7% نيكل), S2 ( 81,8% نحاس, 13,5% المنيوم, 4,7% نيكل) و S3 ( 82,4% نحاس, 13,5% المنيوم, 4,1% نيكل) تم تصنيعها من سبيكة (نحاس-المنيوم-نيكل) الذكية بأستخدام طريقة ميتالورجيا المساحيق مع المعاملة الحرارية. تم إجراء الاختبارات الفيزيائية باستخدام المجهر الضوئي ، المجهر الإلكتروني الماسح وحيود الأشعة السينية للتأكد من وجود طور الأوستينيت قبل المعاملة الحرارية و المارتنسايت بعد المعاملة الحرارية. النتائج بينت ، وجود هذين الطورين في جميع العينات قيد الدراسة. تم أجراء الفحوصات الميكانيكية والتي تضمنت تأثير ذاكرة الشكل وأقصى أنفعال قابل للاستعادة. النتائج بينت أن العينة S3 ( 82,4% نحاس, 13,5% المنيوم, 4,1% نيكل) أعطت أفضل القيم لتأثير ذاكرة الشكل، أقصى أنفعال قابل للاستعادة (5% عند الاستعادة الكاملة) وأقصى أنفعال قابل للأستعادة (10% عند الاستعادة الجزئية).

**الكلمات المفتاحية: ميتالورجيا المساحيق, الأنفعال القابل للأستعادة, تأثير ذاكرة الشكل, سبائك (نحاس-المنيوم-نيكل) الذكية.**